The Improved Comparative Reactivity Method (ICRM): measurements of OH reactivity at high-NO_X conditions in ambient air

Wenjie Wang[1,3#], Jipeng Qi[1,2#], Jun Zhou[1,2], Bin Yuan[1,2*], Yuwen Peng[1,2], Sihang Wang[1,2] Jonathan Williams[4], Vinayak Sinha[5], Min Shao[1,2]

[1]Institute for Environmental and Climate Research, Jinan University, Guangzhou 511443, China.

[2]Guangdong-Hongkong-Macau Joint Laboratory of Collaborative Innovation for Environmental Quality, Guangzhou 511443, China.

[3]Multiphase Chemistry Department, Max Planck Institute for Chemistry, Mainz 55128, Germany.

[4]Atmospheric Chemistry Department, Max Planck Institute for Chemistry, Mainz 55128, Germany.

[5]Department of Earth and Environmental Sciences, Indian Institute of Science Education and Research (IISER), Mohali 140306, India.

#W.J.W. and J.P.Q. contributed equally to this work.

*Correspondence to: byuan@jnu.edu.cn

1. Calculation of X_R

Due to the variation of reagent ion source and sample humidity, the pyrrole (C_4H_5N) ion signal is normalized to a standard reagent ion signal of 10^6 counts/s (cps) as following in Eq. 1.

$$Pyrrole_{ncps} = \frac{i[C_4H_5NH^+] \times 10^6}{i[H_3O^+] + X_R \times i[H_3O^+H_2O]} \tag{1}$$

Where $Pyrrole_{ncps}$ is a normalized signal of the pyrrole, and $i[C_4H_5NH^+]$, $i[H_3O^+]$, and $i[H_3O^+H_2O]$ represent the signals of different product ions, respectively. The value of X_R not only represents difference in detection efficiencies of detector, but also the difference in rate coefficients of the proton transfer reactions H_3O^+ + pyrrole and $H_3O^+(H_2O)$ + pyrrole (de Gouw et al., 2003; de Gouw et al., 2007).

Here, the X_R value of pyrrole was determined by the laboratory experiment. The $i[C_4H_5NH^+]$, $i[H_3O^+]$, and $i[H_3O^+H_2O]$ were measured from a dry (0%) to 100% humidified pyrrole standard gas, respectively. The pyrrole signal become independent of relative humidity when normalized to $i[H_3O^+] + X_R \times i[H_3O^+H_2O]$. In other words, the correlation coefficient (r^2) of relative humidity and normalized pyrrole signal reaches a minimum at the optimized X_R value. This method is inspired by the calculation of enhancement ratios and the source contribution of different species in the previous studies (Millet et al., 2005; Yuan et al., 2010). Figure S1 (a) shows the result of the correlation coefficient of at different X_R with a bin of 0.01 values. We found that r^2 is the smallest when the X_R value is 0. Figure S1 (b) shows the time series of pyrrole signals before and after normalizing to $i[H_3O^+] + X_R \times i[H_3O^+H_2O]$, respectively. It is shown that pyrrole signal reaches a stable level after normalized with the increase of relative humidity. Therefore, the X_R value is determined as 0.

Table S1. The list of all species used to calculate OH reactivity in this study.

Species name	Species name	Species name
Alkanes	n-Undecane	1,2,3-Trimethylbenzene
Ethane	n-Dodecane	p-Diethylbenezen
Propane	**Alkenes**	m-Diethylbenezen
iso-Butane	Ethene	**Alkyne**
n-Butane	Propene	Acetylene
iso-Pentane	cis-2-Butene	**OVOCs**
n-Pentane	trans-2-Butene	Formaldehyde
Cyclopentane	1-Butene	Methanol
2-Methylpentane	1-Pentene	Acetaldehyde
n-Hexane	Isoprene	Ethanol
Cyclohexane	cis-2-Pentene	Acrolein
2,2-Dimethylbutane	trans-2-Pentene	Acetone
2,3-Dimethylbutane	1-Hexene	Propanol
3-Methylpentane	**Aromatics**	Furan
3-Methylhexane	Benzene	MVK+MACR
2,2,4-Trimethylpentane	Toluene	MEK
Methylcyclopentane	Ethylbenzene	Pentanones
n-Heptane	x, p-Xylene	Phenol
Methylcyclohexane	Styrene	2-Furaldehyde
2,3,4-Trimethylpentane	o-Xylene	Benzyl alcohol
2-Methylheptane	n-Propylbenzene	**Inorganics**
3-Methylheptane	isopropylbenzene	CO
2,4-Dimethylpentane	o-Ethyltoluene	NO
2,3-Dimethylpentane	m-Ethyltoluene	NO_2
2-Methylhexane	p-Ethyltoluene	SO_2
n-Octane	1,2,4-Trimethylbenzene	O_3
n-Decane	1,3,5-Trimethylbenzene	

48
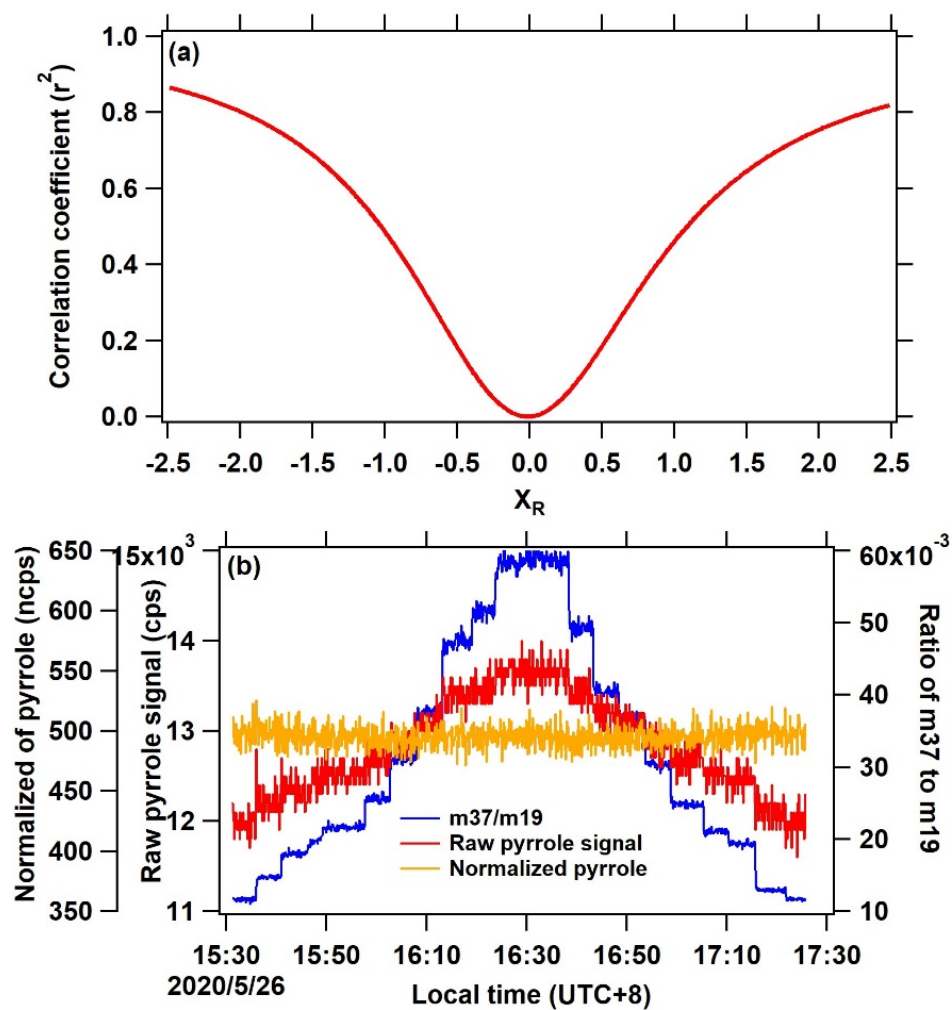
Figure S1. (a) The horizontal represents different X_R values (from -2.5 to 2.5). The vertical represents the correlation coefficient that pyrrole is normalized to H_3O^+ signals and m37/m19 at different X_R values. **(b)** The time series of the signal of pyrrole in cps (red) and in ncps (yellow, normalized to m19 and m37) with the change of humidity (blue, represented as the ratio of m37 to m19).

54
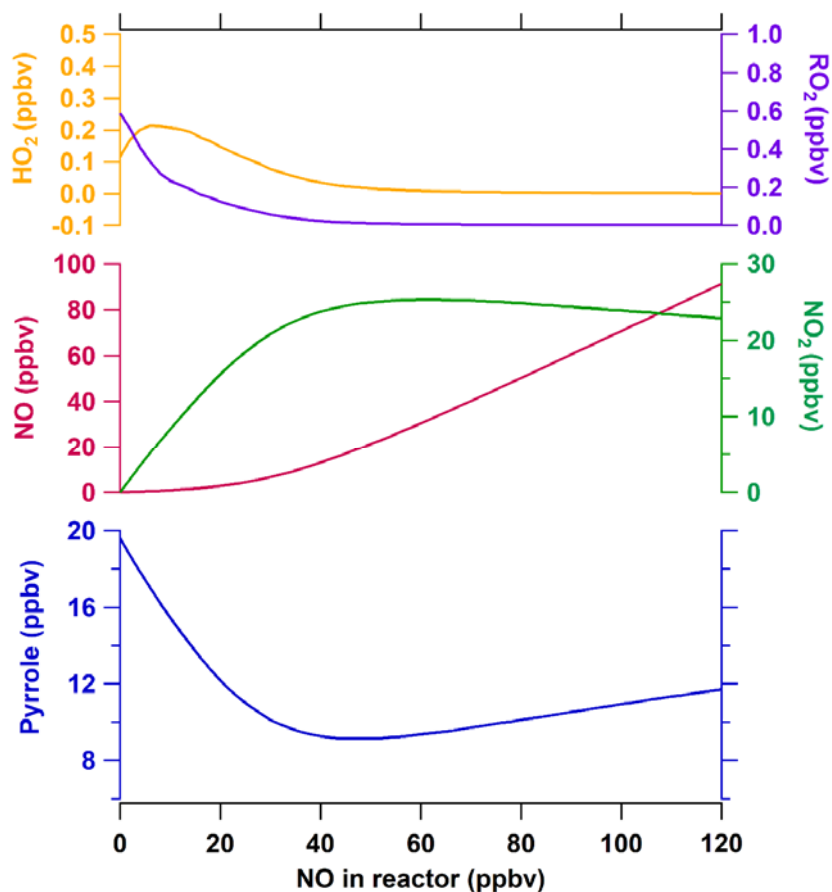
55 **Figure S2**. The remaining concentrations of pyrrole, NO, NO_2, HO_2, and RO_2

56 outflowing of the reactor (with the reaction time of ~ 11 s) as a function of introduced

57 NO in the reactor.

58
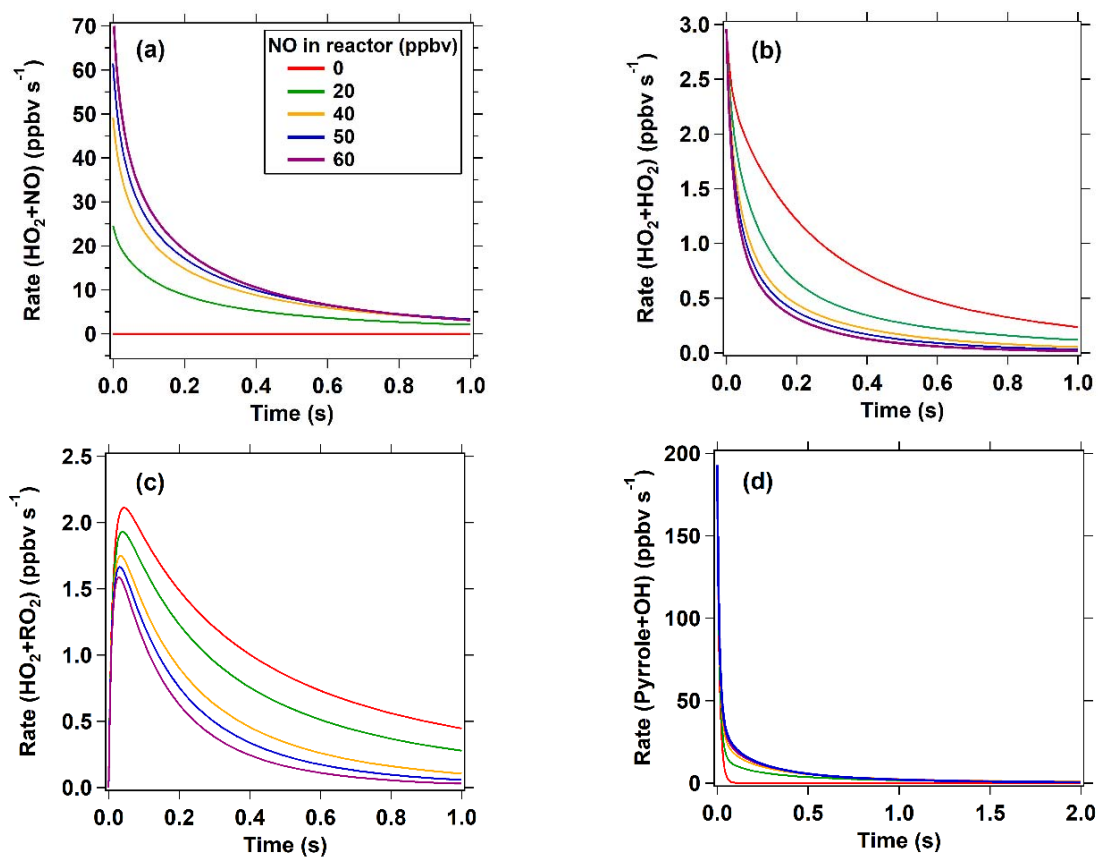
59 **Figure S3.** The reaction rates of HO$_2$+NO, HO$_2$+HO$_2$, HO$_2$+RO$_2$ and Pyrrole+OH as a

60 function of reaction time in the reactor. Four levels of introduced NO concentrations (0,

61 20, 40, 50, 60 ppbv) was selected. The reaction time ranging from 0 to 1s is displayed

62 due to the high reaction rates mainly occurred during this period.

63

64
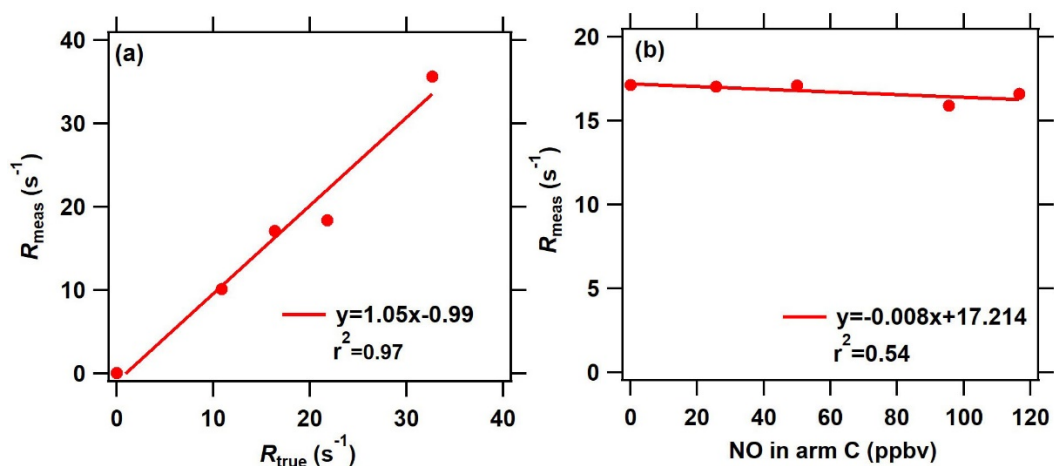
65 **Figure S4**. **(a)** The OH reactivity calibration of NO_2, **(b)** Comparison of measured and

66 true OH reactivity of NO_2 at different NO concentrations introduced through arm C in

67 ICRM system.

68
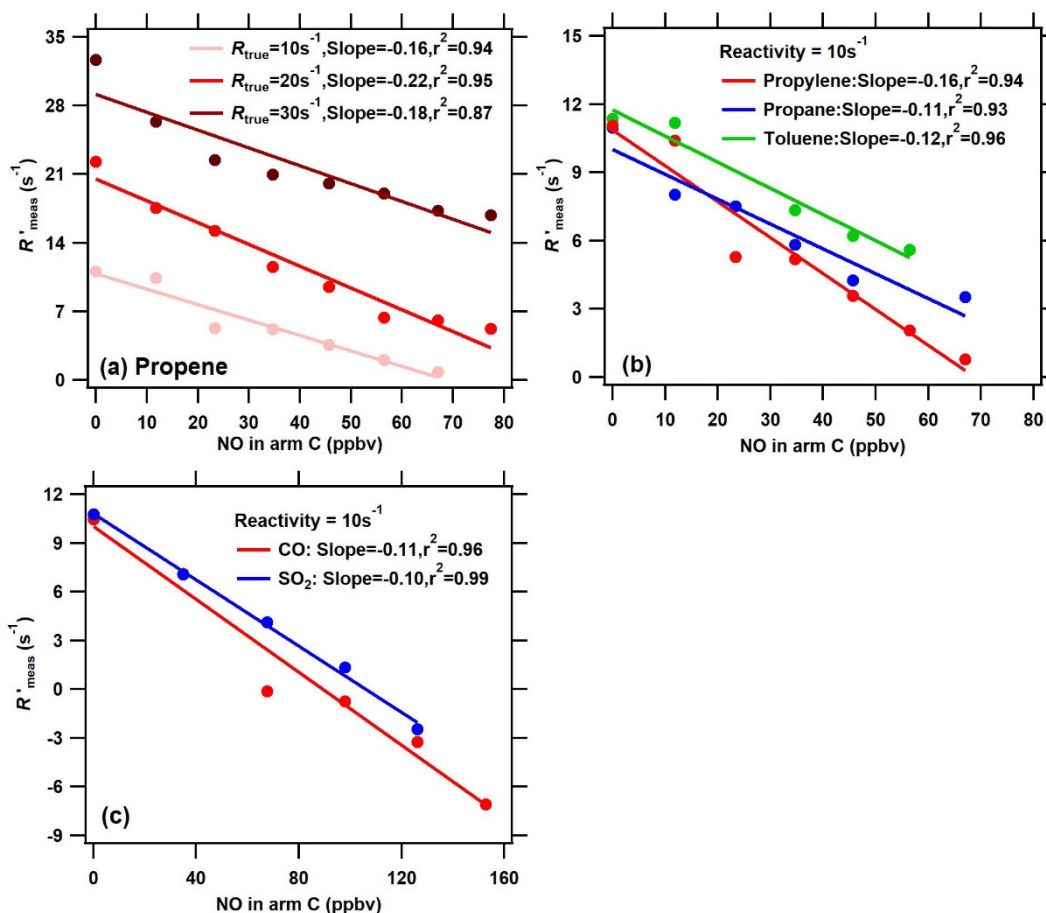
Figure S5. The corrected measured reactivity (R'_{meas}) using the calibration factor α_3 ($R'_{meas} = (\frac{1}{\alpha_3} * R_{meas})$) as a function of NO concentrations at **(a)** different levels of VOCs reactivity for the same species (propene) and **(b)** different VOCs species for the same OH reactivity level (10 s^{-1}); **(c)** The response of the R'_{meas} to NO concentrations at different inorganic species for the same OH reactivity level (10 s^{-1}). The NO, CO, SO$_2$, and VOCs were introduced into the reactor through arm C.

77
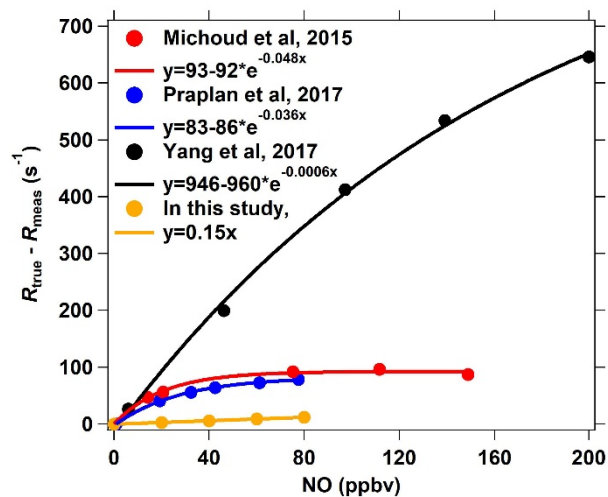
78 **Figure S6**. The effect of NO on the difference between true reactivity and measured

79 OH reactivity (R_{true} - R_{meas}) in the original CRM system. In this study, to correct the

80 systematic deviation at ambient NO=0, the R_{true} - R_{meas} is defined as the difference

81 between true OH reactivity (R_{true}) and the corrected measured OH reactivity (R'_{meas})

82 using the calibration factor α_1 ($R'_{meas} = (\frac{1}{\alpha_1} * R_{meas})$).

83

84 **Figure S7.** Linear correlation between measured and true OH reactivity of propane,

85 CO, and SO$_2$ simulated by box-model.
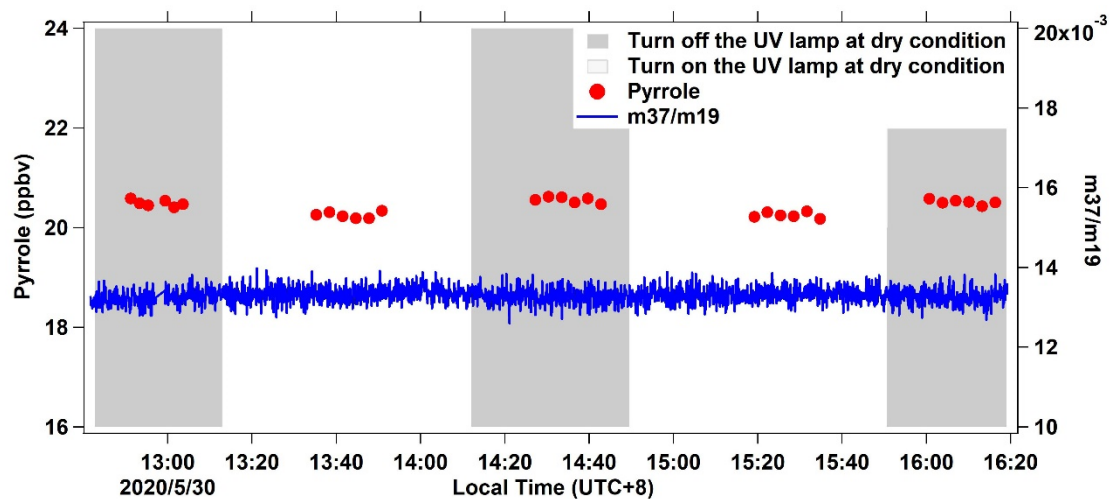
Figure S8. The variation in pyrrole concentration due to photolysis effect in the ICRM system. Two modes were tested by turning on and off the mercury lamp at dry condition (no humidification).
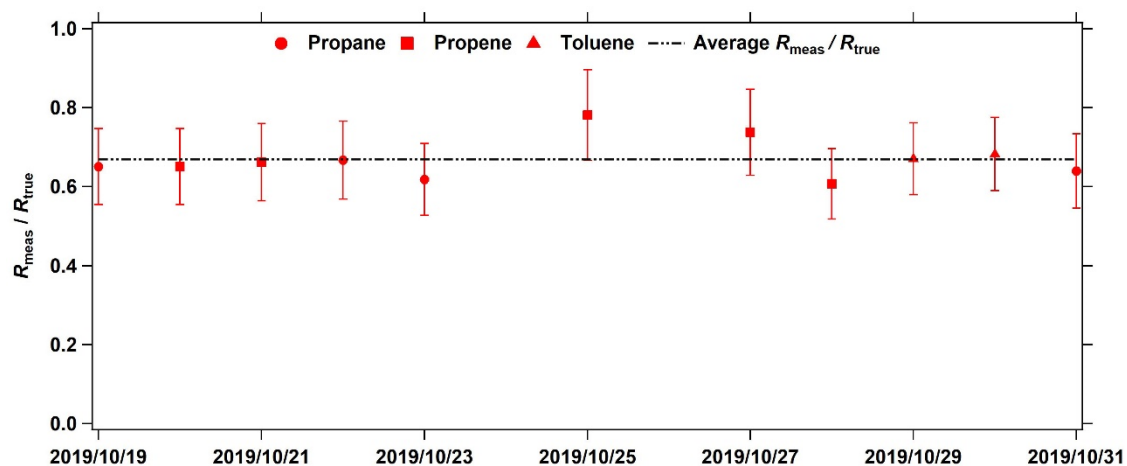
Figure S9. The daily calibration of measured reactivity during the field campaign at Heshan site. The ratio of R_{meas} to R_{true} (R_{meas}/R_{true}) of each day is given. The dashed line represents the average value of R_{meas}/R_{true} during the measurement. Three VOC standard gases (propane, propene and Toluene) were used for the calibration.

References

96

de Gouw, J. and Warneke, C.: Measurements of volatile organic compounds in the earth's atmosphere

98   using proton-transfer-reaction mass spectrometry, Mass Spectrom Rev, 26, 223-257, 2007.

99   de Gouw, J. A., Goldan, P. D., Warneke, C., Kuster, W. C., Roberts, J. M., Marchewka, M., Bertman, S.

100   B., Pszenny, A. A. P., and Keene, W. C.: Validation of proton transfer reaction-mass spectrometry

101   (PTR-MS) measurements of gas-phase organic compounds in the atmosphere during the New

102   England Air Quality Study (NEAQS) in 2002, Journal of Geophysical Research: Atmospheres,

103   108, 2003.

104   Millet, D. B. and Neil M. Donahue, S. N. P., Andrea Polidori, Charles O. Stanier, Barbara J. Turpin,

105   Allen H. Goldstein: Atmospheric volatile organic compound measurements during the Pittsburgh

106   Air Quality Study: Results, interpretation, and quantification of primary and secondary

107   contributions, Journal of Geophysical Research, 110, 1-17, 2005.

108   Yuan, B., Liu, Y., Shao, M., Lu, S., and Streets, D. G.: Biomass Burning Contributions to Ambient

109   VOCs Species at a Receptor Site in the Pearl River Delta (PRD), China, Environmental Science &

110   Technology, 44, 4577-4582, 2010.

111